Spatial electron-photon entanglement

Eitan Kazakevich, Hadar Aharon, and Ofer Kfir*
School of Electrical Engineering, The Iby and Aladar Fleischman Faculty of Engineering, Tel Aviv University, Tel Aviv 69978, Israel

(Received 18 April 2024; revised 25 June 2024; accepted 22 August 2024; published 15 October 2024)

Free electron beams and their quantum coupling with photons are attracting a rising interest due to the basic questions they address and the innovative technology these particles are involved in, such as microscopy, spectroscopy, and quantum computation. This work proposes spatially encoded coupling, where a dual-rail-like electron (e^-) state is entangled to a dual-rail photonic qubit. Thus, it complements the leading current concept of the coupling, which links photonic Fock states with the e^- energy. Importantly, we show that a spatial electron-photon pair can reach maximal entanglement and propose mutually unbiased bases for verifying the entanglement in a realistic experimental apparatus. Although the energy-level coupling of an e^- beam with photonic excitations is well understood, we show that a naïve approach for extending such interaction from a single to a double path results in a retrocausal paradox. In the future, the atomic scale precision of electron microscopes can harness such position-encoded free-e^- entangled qubits for novel quantum sensing and quantum transduction.

DOI: 10.1103/PhysRevResearch.6.043033

I. INTRODUCTION

The phenomenon of entanglement has captured the imagination of physicists since its conception, and now, through the advent of quantum computation and adjacent technologies, it fascinates the broader public as well. Upon its conception, entanglement was used to contest the validity of quantum mechanics by the apparent paradoxes it raises. Famous examples were proposed by Einstein, Podolsky, and Rosen (EPR) [1], and the discussion by Wheeler, Scully, and Drühl on quantum erasers [2,3]. These paradoxes sharpen one's understanding of the quantum nature of entangled particles with respect to locality, realism, and causality. Being a general phenomenon, entanglement is mandatory for quantum computation hardware such as atoms [4,5], ions [6,7], and condensed matter [8,9], as well as for photons [10]. For quantum communication, photons are unique, being the *only suitable fundamental entity* at any scale [11,12].

As free photons, free electrons are fundamental particles—the simplest fermions within the standard model of particle physics. Electron microscopes routinely form high quality electron (e^-) beams and control their parameters such as the kinetic energy, beam size, and convergence angles, combined with optional light insertion and collection apparatuses [13–19]. Even with such a substantial control of a fundamental particle, the concept of entanglement between free electrons and photons has only been conceived recently [20,21]. Thus, free electrons may transduce quantum information, mediating it between a photon and other quantum systems. e^- beams focused to below an angstrom [22] may enable such quantum optical transduction with subatomic selectivity and surpass the diffraction limit of quantum light. Thus, an elaborate effort is made to optimize photonic structures for maximizing and utilizing electron-photon coupling [13,23–28], and to estimate its theoretical supremum across a wide electromagnetic spectral regime [29,30].

Spontaneous transitions involving electron energy-loss spectroscopy (EELS) [31–33], cathodoluminescence (CL) [17,34,35], or both [13,25,36], quantify the coupling directly. They target polaritonic density of states initially at its vacuum level [20,33,37–39] and enable excitations to exhibit quantum statistics such as bunching and antibunching [40–42]. Free electrons couple dominantly through electric fields [13,25,32,33,43–51], so e^--spin effects [52] are typically neglected. In a series of pioneering publications by Potapov, Verbeeck, and co-workers, as well as Sonnentag and Hasselbach, a transversely separated bipartite electron wave function probed coupling to polaritons [53–56]. These experiments analyzed the loss of interference visibility in the far field, tracing out the inaccessible polaritonic degrees of freedom. Complementarily, Remez *et al.* [57] investigated the plasmon-mediated photon emission from a spatially extended e^- wave function, finding that the electron's transverse coherence had no effect on the CL. The role of the plasmons in both cases was quantitative—they offer a high coupling probability, up to a few precent [32,43]. However, among the polaritons, pure photons are key to novel quantum technologies with free-electron beams, where number state [20,25] or quadrature measurements [16,58] can be employed on a distant detector.

The analytic treatment of entanglement between electrons and photons referred, to date, to the energy they exchange along a one-dimensional path of the e^- beam. Approximating

*Contact author: kfir@tauex.tau.ac.il

Published by the American Physical Society under the terms of the Creative Commons Attribution 4.0 International license. Further distribution of this work must maintain attribution to the author(s) and the published article's title, journal citation, and DOI.

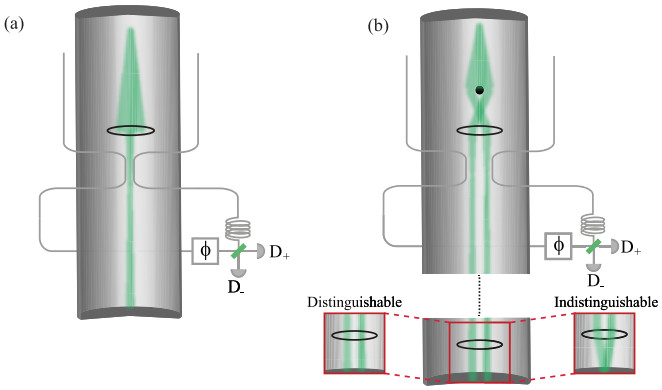


FIG. 1. Scheme of the proposed experiments for single vs double path of free-electron beams. (a) Single path electron coupled to two identical optical waveguides with a phase tuning ϕ and an optional beam splitter. ϕ can be set to direct CL photons strictly to D_+. (b) When the electron beam is in a spatial dual-path superposition both electron and photon states can be controlled: the electrons paths can be detected (left inset) or mixed (right inset).

the e^- path as a line is valid due to the beam's extreme transverse confinement with respect to the optical wavelength. The emphasis on the propagation direction is not accidental. A nonvanishing e^--photon coupling needs a long (μm scale) momentum-matched and uniform interaction, which highlights the importance of the linear e^- path. Importantly, a meaningful entanglement between the e^--energy states and photon generation would necessitate strong coupling amplitudes, which remain elusive [20,24–26]. Furthermore, such entanglement will be challenging to verify even when strong coupling is reached. For example, it is unclear what relevant mutually unbiased bases can be used for electron-state tomography, and alternative proposals for e^- qubits require essentially infinite energy extent [27,59].

Here, we expand the concept of quantum electron-photon coupling to the spatial domain. This work aims at solving two standing conceptual issues: (i) the transition between single and spatially distributed electron state coupled to photons, and (ii) how to test e^--photon entanglement. We pose the problem as a thought experiment in which both particles form dual-rail qubits. Their detection can capture either the populated path or the phase (i.e., sign) between the paths. Since the interaction of spatially encoded states is governed by entanglement, a naïve transverse extension of single-path outputs leads to a causality paradox. We discuss the paradox and its resolution as a two-particle interference, as defined by Jaeger [60]. Importantly, dual-beam e^--photon states can form maximally entangled Bell pairs even in weak-coupling regimes. Thus, this work opens a path for harnessing free electrons as quantum-information carriers, linking the macroscopic scale via the photon to the nanoscale via the electron.

Thought experiment—single e^- path. We examine the properties of the electron-photon coupling in simple geometries. In this section the electron travels on a line equidistant from two parallel single-mode identical waveguides [see Fig. 1(a)], such that the complex coupling amplitude g_{Qu}, which is a geometrical factor, is equal for the two modes. The photon is generated coherently, having its phase temporally locked to the electron timing [58]. As illustrated in Fig. 1(a), we assume that before the interaction region the waveguides are decoupled, separated enough from the electron and from each other. The state of the photon generated in the left/right waveguide is $|1^{\rm ph}_{\rm left/right}\rangle$, respectively, at an implicit narrow linewidth centered around frequency ω. Light is guided to a symmetric beam splitter followed by single-photon detectors marked as D_+ and D_-. Such a setup can be fabricated using integrated silicon-photonics platforms [25,61,62].

Initially, the combined electron-photon state is separable, comprising an electron at its zero-loss energy $|E^e_0\rangle$ and the photonic vacuum,

$$|\psi_1\rangle = |E^e_0\rangle|0^{\rm ph}_{\rm left}, 0^{\rm ph}_{\rm right}\rangle. \tag{1}$$

Assuming the coupling is weak, $|g_{Qu}| \ll 1$, the state after interaction is approximately

$$|\psi_2\rangle \approx |\psi_1\rangle + g_{Qu}|E^e_0 - \hbar\omega\rangle\left(|1^{\rm ph}_{\rm left}, 0^{\rm ph}_{\rm right}\rangle + |0^{\rm ph}_{\rm left}, 1^{\rm ph}_{\rm right}\rangle\right). \tag{2}$$

$|E^e_0 - \hbar\omega\rangle$ represents an e^- energy loss equivalent to one photon $\hbar\omega$, where $\hbar$ is the reduced Plank's constant. A tunable relative phase on one of the optical paths ϕ can direct the symmetric photon state in Eq. (2) to port D_+ after the beam splitter.

Thought experiment—dual-rail e^- qubit. One can extend the above logic to a dual e^- path such that within the interaction region it is in a spatial superposition of two transverse paths, $x = \pm x_0$, overlapping the optical modes [see Fig. 1(b)]. We assume a symmetric apparatus such that both e^- paths have a given coupling amplitude to the adjacent waveguide modes $g^{\rm left}_{Qu} = g^{\rm right}_{Qu} = g_{Qu}$, and negligible coupling to the other. The e^- beam can be smaller than any spatial optical feature, so we neglect the variance of the coupling. The fibers enter an ideal beam splitter and detectors D_+ and D_-, as before.

If done in a transmission electron microscope apparatus, the e^- optics can make the electron paths either distinguishable or indistinguishable, controllably. The path of the electron can be determined by imaging the e^- beams on the e^- camera [Fig. 1(b), left inset]. Alternatively, the e^- paths can be overlapped on the e^- camera to make them indistinguishable. Thus, the user can toggle the indistinguishability of the electron paths to "on" or "off" using the postsample e^- optics.

Thus, turning the indistinguishability on or off seems to allow the photon to end up systematically in the detector D_+, as in the previous section, or not, respectively, since the deterministic interference leading to a photon output at D_+ requires eliminating any which-path information, hence the paradox that the naïve assumptions lead to. It seemingly predicts the manipulation of a particle's probability distribution (the photon) by controlling another (the electron). The paradox emerges from the assumption that the mirror-symmetric initial e^- state forces a particular mirror symmetry on the generated photon. Therefore, detecting the electron either on the left or right (off) results in random hits at D_- and D_+, whereas an indistinguishable e^- path (on), that results in a symmetric dual-rail photon can be set to hit D_+ consistently. Phrasing the paradox as a space-time impossibility, electrons sent to a distant observer would allow him/her to determine

the statistics of the photon detection placed near the interaction point, in a retrocausal manner.

Spatial entanglement as the resolution of the paradox. Clearly, communication is bound by causality. The paradox is resolved since the single and double e^--path effect on a detection at D_+ or D_- is equivalent to the discussion in Jaeger [60] regarding one- and two-particle interference; interferences for one particle emerge only as conditional probabilities with respect to the other. It is equivalent to two-photon polarization or double-path entanglement used for other quantum communication protocols, such as quantum key distribution and quantum eraser [2,3,11,63–65].

To describe the spatially encoded entanglement of the electron and photon pair we follow a similar approach as above [see Eq. (2)] and calculate the electron properties, conditional on measuring the photon at D_+ or D_-. The state prior to the interaction is

$$|\Psi_1\rangle = \frac{1}{\sqrt{2}}\big(|E_0^e, \text{left}\rangle + |E_0^e, \text{right}\rangle\big)|0^{\text{ph}}_{\text{left}}, 0^{\text{ph}}_{\text{right}}\rangle, \tag{3}$$

where now we include the two paths of the electron as different states, at the initial energy. In the weak coupling regime, the state after interaction is

$$|\Psi_2\rangle \approx |\Psi_1\rangle + g_{Qu}\big(|E_{-1}^e, \text{left}\rangle|1^{\text{ph}}_{\text{left}}, 0^{\text{ph}}_{\text{right}}\rangle + |E_{-1}^e, \text{right}\rangle|0^{\text{ph}}_{\text{left}}, 1^{\text{ph}}_{\text{right}}\rangle\big), \tag{4}$$

where the e^- energy lowered by one photon quantum, $E_0^e - \hbar\omega$, is abbreviated as E_{-1}^e. We define the symmetric [as in Eq. (2)] and antisymmetric photonic states $|\pm_{\text{ph}}\rangle = \frac{1}{\sqrt{2}}(|1^{\text{ph}}_{\text{left}}, 0^{\text{ph}}_{\text{right}}\rangle \pm |0^{\text{ph}}_{\text{left}}, 1^{\text{ph}}_{\text{right}}\rangle)$ such that $|1^{\text{ph}}_{\text{left}}, 0^{\text{ph}}_{\text{right}}\rangle = \frac{1}{\sqrt{2}}(|+_{\text{ph}}\rangle + |-_{\text{ph}}\rangle)$ and $|0^{\text{ph}}_{\text{left}}, 1^{\text{ph}}_{\text{right}}\rangle = \frac{1}{\sqrt{2}}(|+_{\text{ph}}\rangle - |-_{\text{ph}}\rangle)$. Since we assume that each waveguide supports a single mode, the beam splitter can be set to fully couple the state $|+_{\text{ph}}\rangle$ to detector D_+, and $|-_{\text{ph}}\rangle$ to D_-. Thus

$$|\Psi_2\rangle \approx |\Psi_1\rangle + g_{Qu}\begin{bmatrix} |E_{-1}^e, \text{left}\rangle(|+_{\text{ph}}\rangle + |-_{\text{ph}}\rangle)/\sqrt{2} \\ + |E_{-1}^e, \text{right}\rangle(|+_{\text{ph}}\rangle - |-_{\text{ph}}\rangle)/\sqrt{2}\end{bmatrix}. \tag{5}$$

The unscattered e^- state, $|\Psi_1\rangle$, can be realistically removed although it is the dominant term, either by software, through postselection of only electron-photon coincidences, or by hardware, by filtering the e^- energy to collect electrons that lost one photon-energy quantum, or by a combination of both. The generation rate of e^--photon pairs scales with $|g_{Qu}|^2$. Furthermore, the symmetric and antisymmetric e^- states can be written similarly, as $|\pm_e\rangle = \frac{1}{\sqrt{2}}(|E_{-1}^e, \text{left}\rangle \pm |E_{-1}^e, \text{right}\rangle)$. Thus, for such postselection Eq. (5) can be reorganized as

$$|\Psi_3\rangle = (|+_{ph}\rangle\,|+_e\rangle + |-_{\text{ph}}\rangle\,|-_e\rangle), \tag{6}$$

and the spatial entanglement between the electron and the photon becomes clear in this Bell-pair form. The symmetric and antisymmetric electron's wave function correlate with the photon detection: $|+_e\rangle$ for hits in D_+ and $|-_e\rangle$ for D_-. If an e^--path mixer that discerns between $|+_e\rangle$ and $|-_e\rangle$ would exist, we could measure the correlations in two mutually unbiased bases: the electron and photon paths would correlate at the left or right positions according to Eq. (4), or alternatively,

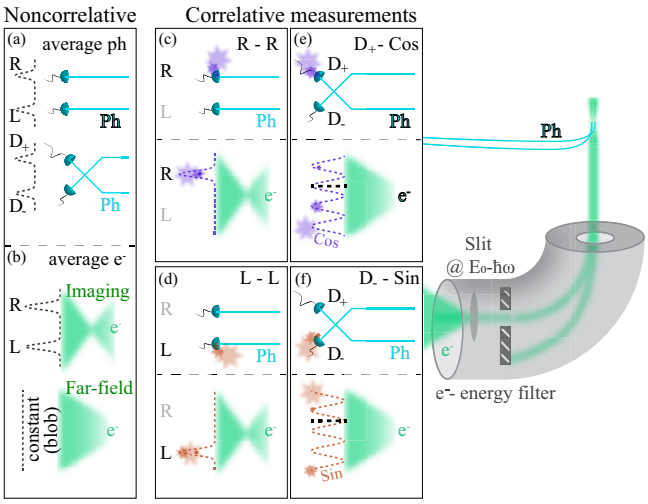


FIG. 2. Expected electron-photon correlations. (a) Measurement probabilities are equally distributed across photonic path (L vs R) or relative phase (D_+ vs D_-), and (b) similarly across the electron path, for imaging and far field modalities. (c), (d) Correlations would emerge between the detected paths of the photon and electron, either L-L or R-R. (e), (f) Entanglement produces conditional e^- diffraction, forming $\cos^2$ or $\sin^2$ patterns when codetected with a photon at D_+ or D_-, respectively.

the hypothetic e-state mixer $|\pm_e\rangle$ would enable coincidences of $|+_{\text{ph}}\rangle$ and $|-_{\text{ph}}\rangle$ with D_+ and D_-, respectively. This resolves the paradox explicitly since the outputs at any selected basis is a random process with equal probabilities. Correlations exist only when comparing the result of coincident events. Thus, causality is maintained since an event-by-event comparison requires a classical communication channel.

Realistic experimental setup for detecting spatial electron-photon entanglement. We now turn to address spatial electron-photon entanglements in a realistic experimental instrument such as an electron microscope (see Fig. 2). The photon system is already feasible. Photons emanating from waveguides interacting with grazing electron beams were measured by Feist *et al.* [25], including their correlation with the electron's energy loss. For the photons, an extension to dual-rail waveguides is straightforward. The challenge is the combination with a dual-rail e^- qubit. Thus, we focus on an electron subsystem that discerns $|+_e\rangle$ from $|-_e\rangle$. We define a unitary propagator for the e^- beam to the detector (e.g., camera) as $\hat{U}^e_{\text{img/ff}}$. The projection either maps of the interaction plane or its far field on the detector, marked as the subindex "img" or "ff," respectively. The final electron-photon state becomes

$$|\Psi_4\rangle = \hat{U}_i^e|\Psi_3\rangle. \tag{7}$$

Thus, the probability for detecting an electron at x_{cam} conditional on photon detection in D_+ and D_- is

$$P(x_{\text{cam}}|D_\pm) = \frac{\langle\Psi_4|\pm_{\text{ph}}, x_{\text{cam}}\rangle\langle\pm_{\text{ph}}, x_{\text{cam}}|\Psi_4\rangle}{|\langle\pm_{\text{ph}}|\Psi_4\rangle|^2}, \text{ or}$$

$$P(x_{\text{cam}}|D_\pm) = \big|\langle x_{\text{cam}}|\hat{U}_i^e|\pm_e\rangle\big|^2. \tag{8}$$

The dual-rail e^- qubit is approximated here as two spatial delta functions on the x axis, $|E^e_{-1}, \text{left}\rangle = \delta(x + x_0)$ and $|E^e_{-1}, \text{right}\rangle = \delta(x - x_0)$. When set to imaging, the propagator $\hat{U}^e_{\text{img}}$ maps any wave function at the interaction region $\psi(x)$ onto a magnified replica with the probability $|\psi(ax_{\text{cam}})|^2$, where $1/a$ is the magnification factor. Thus, for any e^--detection position $ax_{\text{cam}} = \pm x_0$, the probabilities for photon detection at D_+ or D_- are equal [Eq. (8)], regardless of the phase between the left and right paths. Alternatively, when set to far field, the propagator $\hat{U}^e_{\text{ff}}$ projects the Fourier transform on camera, $\mathcal{F}[\psi(x)]_{\{k_x\}}$. Each spatial frequency k_x is mapped by the e^--optics lensing system to $x_{\text{cam}}/\lambda_{\text{DB}}L_c$, where λ_{DB} is the de Broglie wavelength and L_c is the effective camera length. The far field of the e^- delta pair is a sinusoidal probability pattern. Thus, detections at D_+ and D_- would correlate with a squared cosine and sine e^--probability patterns,

$$P(x_{\text{cam}}|D_+) = \cos^2\left(2x_0\frac{x_{\text{cam}}}{\lambda_{\text{DB}}L_c}\right), \tag{9}$$

$$P(x_{\text{cam}}|D_-) = \sin^2\left(2x_0\frac{x_{\text{cam}}}{\lambda_{\text{DB}}L_c}\right). \tag{10}$$

Thus photon detections fully correlate with the shift of the conditional harmonic e^- pattern. Considering the paradox, if the person detecting the electrons has no event-by-event information on the photonic side, effectively tracing out the photonic state, the e^- probability spans a uniform pattern (blob) in the far field or random hits on the magnified image of the left/right paths. In other words, no information can be extracted by any side individually.

II. DISCUSSION

The electron-photon entanglement can be viewed from the perspective of spatial symmetry. The physical system is unchanged under mirror transformation, $x \to -x$, so the allowed parity eigenvalues for the quantum states are ± 1. Assuming an initially symmetric e^- state [e.g., Eq. (3)], the parity of a final electron-photon state is $+1$, so either both are positive or both are negative, symmetric, or antisymmetric, respectively. Since a antisymmetric photon hits D_+ and an asymmetric hits D_-, it coincides with a symmetric or antisymmetric e^- wave function, respectively. These ± 1 eigenvalues are a binary measurement basis, such as a two-level system or photon polarization. Postselecting at detector positions $2x_0\frac{x_{\text{cam}}}{\lambda_{\text{DB}}L_c} = n\pi/2$ provides a definite binary measurement, where n is an integer. e^- hits at positions with even (or odd) n values are interpreted as $+1$ (or -1) since they are deterministically from the symmetric (or antisymmetric) e^- state. Once these parallels are clearly drawn, they can be quite powerful. One can envision extending protocols for Bell states to e^--photon pairs.

Figure 3 presents the von Neumann entanglement entropy of the e^--photon pair (blue), as well as the effect of parasitic cross-path coupling vs the spacing between the two electron trajectories (red). It is based on experimentally measured rates for CL photons at a wavelength of $\lambda_{\text{ph}} = 1550\,\text{nm}$ (see Fig. 4D in Ref. [25]). The calculation is for a spacing of λ_{ph} between the inner surfaces of the waveguides. When the e^--path spacing d is small, $d \ll \lambda_{\text{ph}}$, the states are separable, having zero entanglement entropy. Additionally, the ratio of parasitic

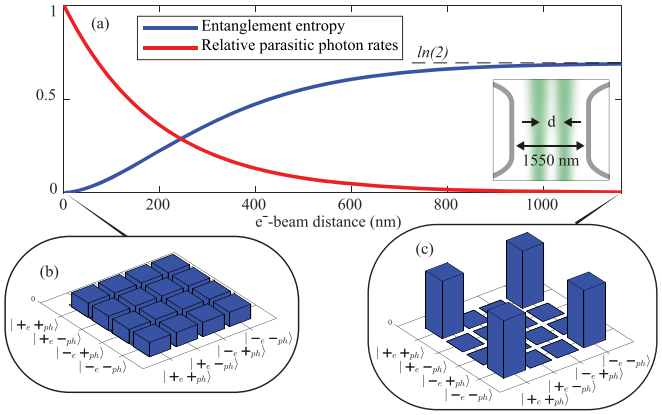


FIG. 3. (a) The entanglement entropy and the relative cross-coupling rates vs the distance of the e^- beam, d, for a waveguide spacing of one infrared wavelength (see inset), based on the experimental data in Ref. [25]. Panels (b) and (c) are the density matrices for overlapping and well separated e^- paths.

vs proper coupling to the adjacent waveguide approaches unity. For the exemplary parameters chosen here, when each e^- path approaches the surface of its adjacent waveguides the parasitic coupling drops by four orders of magnitude. Thus, the electron-photon pair becomes maximally entangled, with an entropy reaching $\ln 2$, for events where both an electron and a photon were detected. These are electron-photon Bell pairs. This scheme may be extendable to multipartite entanglement by using additional spatial paths. Furthermore, using the mature quantum optics and e^- optics technologies, these e^--photon pairs may transduce quantum information between the macroscopic world and individual quantum systems, with atomic-scale precision.

III. CONCLUSION

We reviewed the phenomenon of electron-photon coupling for dual-rail spatial states. We present the analog between the excitation of two photonic modes by a single vs double e^- path and one-particle vs two-particle interference, as defined by Jaeger *et al.* [60]. In analyzing the entanglement between the spatially encoded e^- and photon dual-rail qubits we propose an experimental approach to verify their entanglement and show that the resulting e^--photon pairs can be maximally entangled. This work outlines the requirements for realizing this entanglement test in a realistic apparatus. In principle, this would enable a demonstration of two-particle interference with different fundamental entities, however as Wheeler stated, "no phenomenon is a phenomenon until it is an observed phenomenon." In the future, these qubitlike spatial states of the electron can be the backbone of quantum computation hardware or precision quantum sensing based on free electrons, that exchange quantum information by the photons they release.

ACKNOWLEDGMENTS

O.K. gratefully acknowledges the Young Faculty Award from the National Quantum Science and Technology program of the Israeli Planning and Budgeting Committee. H.A.

gratefully acknowledges the Excellent Student Scholarship from the Center for Quantum Science and Technology at Tel Aviv University. This research was supported by the Israel Science Foundation (Grant No. 1021/22).

[1] A. Einstein, B. Podolsky, and N. Rosen, Can quantum-mechanical description of physical reality be considered complete? Phys. Rev. **47**, 777 (1935).

[2] J. A. Wheeler, The "past" and the "delayed-choice" double-slit experiment, in *Mathematical Foundations of Quantum Theory*, edited by A. R. Marlow (Academic, New York, 1978), pp. 9–48.

[3] M. O. Scully and K. Drühl, Quantum eraser: A proposed photon correlation experiment concerning observation and "delayed choice" in quantum mechanics, Phys. Rev. A **25**, 2208 (1982).

[4] D. Bluvstein, H. Levine, G. Semeghini, T. T. Wang, S. Ebadi, M. Kalinowski, A. Keesling, N. Maskara, H. Pichler, M. Greiner, V. Vuletić, and M. D. Lukin, A quantum processor based on coherent transport of entangled atom arrays, Nature (London) **604**, 451 (2022).

[5] K. Wintersperger, F. Dommert, T. Ehmer, A. Hoursanov, J. Klepsch, W. Mauerer, G. Reuber, T. Strohm, M. Yin, and S. Luber, Neutral atom quantum computing hardware: Performance and end-user perspective, EPJ Quantum Technol. **10**, 32 (2023).

[6] C. D. Bruzewicz, J. Chiaverini, R. McConnell, and J. M. Sage, Trapped-ion quantum computing: Progress and challenges, Appl. Phys. Rev. **6**, 021314 (2019).

[7] T. Manovitz, Y. Shapira, L. Gazit, N. Akerman, and R. Ozeri, Trapped-ion quantum computer with robust entangling gates and quantum coherent feedback, PRX Quantum **3**, 010347 (2022).

[8] S. Cao *et al.*, Generation of genuine entanglement up to 51 superconducting qubits, Nature (London) **619**, 7971 (2023).

[9] S. Storz *et al.*, Loophole-free bell inequality violation with superconducting circuits, Nature (London) **617**, 7960 (2023).

[10] L. S. Madsen *et al.*, Quantum computational advantage with a programmable photonic processor, Nature (London) **606**, 7912 (2022).

[11] J. Yin *et al.*, Satellite-to-ground entanglement-based quantum key distribution, Phys. Rev. Lett. **119**, 200501 (2017).

[12] X.-S. Ma *et al.*, Quantum teleportation over 143 kilometres using active feed-forward, Nature (London) **489**, 7415 (2012).

[13] N. Varkentina *et al.*, Cathodoluminescence excitation spectroscopy: Nanoscale imaging of excitation pathways, Sci. Adv. **8**, eabq4947 (2022).

[14] R. Shiloh, T. Chlouba, and P. Hommelhoff, Quantum-coherent light-electron interaction in a scanning electron microscope, Phys. Rev. Lett. **128**, 235301 (2022).

[15] R. Dahan *et al.*, Resonant phase-matching between a light wave and a free-electron wavefunction, Nat. Phys. **16**, 11 (2020).

[16] J. H. Gaida, H. Lourenço-Martins, M. Sivis, T. Rittmann, A. Feist, F. J. García de Abajo, and C. Ropers, Attosecond electron microscopy by free-electron homodyne detection, Nat. Photonics **18**, 509 (2024).

[17] T. Coenen, E. J. R. Vesseur, and A. Polman, Angle-resolved cathodoluminescence spectroscopy, Appl. Phys. Lett. **99**, 143103 (2011).

[18] A. Arbouet, G. M. Caruso, and F. Houdellier, Ultrafast transmission electron microscopy: Historical development, instrumentation, and applications, in *Advances in Imaging and Electron Physics* (Elsevier, New York, 2018), pp. 1–72.

[19] D. R. Cremons, D. A. Plemmons, and D. J. Flannigan, Defect-mediated phonon dynamics in TaS_2 and WSe_2, Struct. Dyn. **4**, 044019 (2017).

[20] O. Kfir, Entanglements of electrons and cavity-photons in the strong coupling regime, Phys. Rev. Lett. **123**, 103602 (2019).

[21] V. D. Giulio, M. Kociak, and F. J. G. de Abajo, Probing quantum optical excitations with fast electrons, Optica **6**, 1524 (2019).

[22] S. J. Pennycook and P. D. Nellist, *Scanning Transmission Electron Microscopy: Imaging and Analysis*, 1st ed. (Springer, New York, 2011).

[23] G. Huang, N. J. Engelsen, O. Kfir, C. Ropers, and T. J. Kippenberg, Electron-photon quantum state heralding using photonic integrated circuits, PRX Quantum **4**, 020351 (2023).

[24] Y. D'Mello, R. Dahan, S. Bernal, X. Shi, I. Kaminer, and D. V. Plant, Efficient coupling between free electrons and the supermode of a silicon slot waveguide, Opt. Express **31**, 19443 (2023).

[25] A. Feist *et al.*, Cavity-mediated electron-photon pairs, Science **377**, 777 (2022).

[26] M. Bézard, I. Si Hadj Mohand, L. Ruggierio, A. Le Roux, Y. Auad, P. Baroux, L. H. G. Tizei, X. Checoury, and M. Kociak, High efficiency coupling of free electrons to sub-λ^3 modal volume, high-Q photonic cavities, ACS Nano **18**, 10417 (2024).

[27] R. Dahan, G. Baranes, A. Gorlach, R. Ruimy, N. Rivera, and I. Kaminer, Creation of optical cat and GKP states using shaped free electrons, Phys. Rev. X **13**, 031001 (2023).

[28] A. Karnieli, C. Roques-Carmes, N. Rivera, and S. Fan, Strong coupling and single-photon nonlinearity in free-electron quantum optics, ACS Photon. **11**, 3401 (2024).

[29] Z. Zhao, Upper bound for the quantum coupling between free electrons and photons, arXiv:2404.01221.

[30] Z. Xie, Z. Chen, H. Li, Q. Yan, H. Chen, X. Lin, I. Kaminer, O. D. Miller, and Y. Yang, Maximal quantum interaction between free electrons and photons, arXiv:2404.00377.

[31] R. F. Egerton, *Electron Energy-Loss Spectroscopy in the Electron Microscope* (Springer, Boston, 1995).

[32] J. Nelayah, M. Kociak, O. Stéphan, F. J. García de Abajo, M. Tencé, L. Henrard, D. Taverna, I. Pastoriza-Santos, L. M. Liz-Marzán, and C. Colliex, Mapping surface plasmons on a single metallic nanoparticle, Nat. Phys. **3**, 348 (2007).

[33] H. Lourenço-Martins, P. Das, L. H. G. Tizei, R. Weil, and M. Kociak, Self-hybridization within non-hermitian localized plasmonic systems, Nat. Phys. **14**, 360 (2018).

[34] A. Polman, M. Kociak, and F. J. García de Abajo, Electron-beam spectroscopy for nanophotonics, Nat. Mater. **18**, 1158 (2019).

[35] M. Zhao, M. Bosman, M. Danesh, M. Zeng, P. Song, Y. Darma, A. Rusydi, H. Lin, C.-W. Qiu, and K. P. Loh, Visible surface plasmon modes in single Bi_2Te_3 nanoplate, Nano Lett. **15**, 8331 (2015).

[36] S. Yanagimoto, N. Yamamoto, T. Yuge, H. Saito, K. Akiba, and T. Sannomiya, Time-correlated electron and photon counting microscopy, Commun. Phys. **6**, 260 (2023).

[37] S. Meuret, T. Coenen, S. Y. Woo, Y.-H. Ra, Z. Mi, and A. Polman, Nanoscale relative emission efficiency mapping using cathodoluminescence $g^{(2)}$ imaging, Nano Lett. **18**, 2288 (2018).

[38] S. Meuret, L. H. G. Tizei, T. Auzelle, R. Songmuang, B. Daudin, B. Gayral, and M. Kociak, Lifetime measurements well below the optical diffraction limit, ACS Photonics **3**, 1157 (2016).

[39] P. Schattschneider and H. Lichte, Correlation and the density-matrix approach to inelastic electron holography in solid state plasmas, Phys. Rev. B **71**, 045130 (2005).

[40] L. H. G. Tizei and M. Kociak, Spatially resolved quantum nano-optics of single photons using an electron microscope, Phys. Rev. Lett. **110**, 153604 (2013).

[41] S. Meuret, L. H. G. Tizei, T. Cazimajou, R. Bourrellier, H. C. Chang, F. Treussart, and M. Kociak, Photon bunching in cathodoluminescence, Phys. Rev. Lett. **114**, 197401 (2015).

[42] M. Scheucher, T. Schachinger, T. Spielauer, M. Stöger-Pollach, and P. Haslinger, Discrimination of coherent and incoherent cathodoluminescence using temporal photon correlations, Ultramicroscopy **241**, 113594 (2022).

[43] F. J. García de Abajo, Optical excitations in electron microscopy, Rev. Mod. Phys. **82**, 209 (2010).

[44] X. Li, G. Haberfehlner, U. Hohenester, O. Stéphan, G. Kothleitner, and M. Kociak, Three-dimensional vectorial imaging of surface phonon polaritons, Science **371**, 1364 (2021).

[45] Y. Kurman *et al.*, Spatiotemporal imaging of 2D polariton wave packet dynamics using free electrons, Science **372**, 1181 (2021).

[46] M. Taleb, M. Hentschel, K. Rossnagel, H. Giessen, and N. Talebi, Phase-locked photon–electron interaction without a laser, Nat. Phys. **19**, 869 (2023).

[47] Y. Yang, C. Roques-Carmes, S. E. Kooi, H. Tang, J. Beroz, E. Mazur, I. Kaminer, J. D. Joannopoulos, and M. Soljačić, Photonic flatband resonances for free-electron radiation, Nature (London) **613**, 7942 (2023).

[48] A. Karnieli, D. Roitman, M. Liebtrau, S. Tsesses, N. Van Nielen, I. Kaminer, A. Arie, and A. Polman, Cylindrical metalens for generation and focusing of free-electron radiation, Nano Lett. **22**, 5641 (2022).

[49] A. Konečná, F. Iyikanat, and F. J. García de Abajo, Entangling free electrons and optical excitations, Sci. Adv. **8**, eabo7853 (2022).

[50] N. van Nielen, M. Hentschel, N. Schilder, H. Giessen, A. Polman, and N. Talebi, Electrons generate self-complementary broadband vortex light beams using chiral photon sieves, Nano Lett. **20**, 5975 (2020).

[51] A. Karnieli, N. Rivera, A. Arie, and I. Kaminer, The coherence of light is fundamentally tied to the quantum coherence of the emitting particle, Sci. Adv. **7**, eabf8096 (2021).

[52] N. Talebi and I. Březinová, Exchange-mediated mutual correlations and dephasing in free-electrons and light interactions, New J. Phys. **23**, 063066 (2021).

[53] J. Verbeeck, D. van Dyck, H. Lichte, P. Potapov, and P. Schattschneider, Plasmon holographic experiments: Theoretical framework, Ultramicroscopy **102**, 239 (2005).

[54] P. L. Potapov, H. Lichte, J. Verbeeck, and D. van Dyck, Experiments on inelastic electron holography, Ultramicroscopy **106**, 1012 (2006).

[55] P. L. Potapov, J. Verbeeck, P. Schattschneider, H. Lichte, and D. van Dyck, Inelastic electron holography as a variant of the feynman thought experiment, Ultramicroscopy **107**, 559 (2007).

[56] P. Sonnentag and F. Hasselbach, Measurement of decoherence of electron waves and visualization of the quantum-classical transition, Phys. Rev. Lett. **98**, 200402 (2007).

[57] R. Remez, A. Karnieli, S. Trajtenberg-Mills, N. Shapira, I. Kaminer, Y. Lereah, and A. Arie, Observing the quantum wave nature of free electrons through spontaneous emission, Phys. Rev. Lett. **123**, 060401 (2019).

[58] O. Kfir, V. Di Giulio, F. J. G. de Abajo, and C. Ropers, Optical coherence transfer mediated by free electrons, Sci. Adv. **7**, eabf6380 (2021).

[59] O. Reinhardt, C. Mechel, M. Lynch, and I. Kaminer, Free-electron qubits, Ann. Phys. **533**, 2000254 (2021).

[60] G. Jaeger, M. A. Horne, and A. Shimony, Complementarity of one-particle and two-particle interference, Phys. Rev. A **48**, 1023 (1993).

[61] J.-W. Henke *et al.*, Integrated photonics enables continuous-beam electron phase modulation, Nature (London) **600**, 7890 (2021).

[62] Y. Yang, P. Cattaneo, A. S. Raja, B. Weaver, R. N. Wang, A. Sapozhnik, F. Carbone, T. LaGrange, and T. J. Kippenberg, Unifying frequency metrology across microwave, optical, and free-electron domains, arXiv:2403.10486.

[63] T. J. Herzog, P. G. Kwiat, H. Weinfurter, and A. Zeilinger, Complementarity and the quantum eraser, Phys. Rev. Lett. **75**, 3034 (1995).

[64] S. P. Walborn, M. O. Terra Cunha, S. Pádua, and C. H. Monken, Double-slit quantum eraser, Phys. Rev. A **65**, 033818 (2002).

[65] D. Ribezzo *et al.*, Quantum key distribution over 100 km of underwater optical fiber assisted by a fast-gated single-photon detector, Phys. Rev. Appl. **20**, 044052 (2023).